Collar Rot of Grapevine Caused by a Novel *Pleiocarpon* Lineage in Peru

Luis A. Álvarez *, Gabriela Salcedo-Astorima, Phillip Ormeño-Vásquez, Naysha Rojas-Villa, José Soto-Heredia

Posted Date: 6 May 2026

doi: 10.20944/preprints202605.0304.v1

Keywords: *Cylindrocarpon*-like fungi; black foot; salt creek rootstock; *Vitis vinifera*

 doi:10.20944/preprints202605.0304.v1

Article

Collar Rot of Grapevine Caused by a Novel *Pleiocarpon* Lineage in Peru

Luis A. Álvarez [1,2,*], Gabriela Salcedo-Astorima [1], Phillip Ormeño-Vásquez1 [2,3], Naysha Rojas-Villa [1,2] and José Soto-Heredia [4]

[1] Facultad de Ciencias Agrarias, Universidad Nacional de Cañete. Jr. San Agustín 124, San Vicente de Cañete, Cañete – Lima, Peru

[2] Grupo Agrobiotecnológico de la Costa Peruana. San Vicente de Cañete, Cañete – Lima, Peru

[3] Facultad de Agronomía y Sistemas Naturales y Facultad de Ciencias Biológicas de la Universidad Pontificia Católica de Chile.

[4] Departamento Académico de Fitopatología, Facultad de Agronomía – Universidad Nacional Agraria La Molina, apartado postal 12-056 – La Molina, Lima Perú

* Correspondence: lalvarez@undc.edu.pe; +51 994053327

Abstract

Severe decline and death of young table grape vines (1 to 2 years old) have been observed recurrently in commercial vineyards in Peru since 2022. Affected plants developed rapid shoot wilting associated with extensive necrotic lesions at the rootstock collar below the graft union, leading to plant death within days of symptom onset. A *Cylindrocarpon*-like fungus was consistently isolated from symptomatic collar tissues. Morphological characterization, cardinal temperature assays, and phylogenetic analyses based on the internal transcribed spacer region (ITS) and histone H3 (*his3*) gene identified the pathogen as a member of the genus *Pleiocarpon*. Bayesian inference of concatenated sequences resolved the Peruvian isolates as a distinct lineage sister to *P. strelitziae* (posterior probability = 1.00). Greenhouse pathogenicity tests with two representative isolates on cv. Red Globe grafted onto Salt Creek rootstock reproduced collar lesions and shoot wilting, fulfilling Koch's postulates. Optimal mycelial growth occurred between 25.7 to 26.1 °C, and maximum experimental growth was observed between 28.8 to 31.5 °C, consistent with warm conditions during vineyard establishment in coastal Peru. The disease, designated here as collar rot of grapevine, is pathologically distinct from classical black-foot disease due to its extensive belowground collar necrosis and rapid vine collapse. Recurrent outbreaks and the near-exclusive use of the susceptible Salt Creek rootstock indicate that *Pleiocarpon*-associated collar rot is an emerging threat to table grape production in Peru.

Keywords: *Cylindrocarpon*-like fungi; black foot; salt creek rootstock; *Vitis vinifera*

1. Introduction

Grapevine (*Vitis vinifera* L.) is extensively cultivated in Peru, mainly for table grapes, wine production, and for the distillation of grape brandy known as "Pisco" [1]. Over recent decades, Peru has consolidated its position as the leading global exporter of table grapes for the third consecutive year, with export volumes achieving 870,000 t during the 2025–2026 campaign [2]. National production is mainly concentrated in the coastal regions of Ica and Piura, which account for 49% and 36% of the national volume, respectively [3]. This export campaign generally extends from October to April and includes more than 56 varieties of table grapes.

In late summer 2022, symptoms of decline and death of young grapevine plants (1–2 years after planting) of unknown etiology, were observed in commercial vineyards in the Piura region. Affected plants exhibited wilting and eventually died, resulting in severe plant losses in the fields. Necrotic lesions were regularly observed belowground at the rootstock collar, particularly in the buried

 doi:10.20944/preprints202605.0304.v1

portion below the graft union. Because such collar lesions are uncommon in grapevines, this condition was provisionally designated as collar rot of grapevines.

In subsequent years, similar symptoms were observed during late spring and, more frequently, throughout the summer in Piura and other commercial grape-growing regions of Peru. However, the impact of this syndrome on young grapevine plants has not yet been thoroughly investigated.

Soil-borne pathogens, such as *Fusarium* spp., are associated with root and crown rot, vascular wilt, basal rot, and wood cankers in declining grapevines in both young and mature vineyards worldwide [4–6].

Spies et al. [7] reported the pathogenicity of oomycetes, including *Pythium* (*P. vexans*, *P. ultimum*, and *P. irregulare*) and *Phytophthora* (*Ph. cinnamomi* and *Ph. niederhauserii*), which are associated with crown and root rot of grapevines in South Africa. In that study, isolates of *Ph. cinnamomi* were the most aggressive, followed by those of *Ph. niederhauserii* and *P. vexans.*

In Peru, table grape production is concentrated along the hyper-arid Pacific coast, where desert conditions and extremely low annual rainfall prevail [8]. Abiotic stress factors, particularly drought and high temperatures, predispose grapevines to several economically important diseases that affect both their productivity and longevity. Among these, grapevine trunk diseases are a constant threat [9,10]. In Peru, this complex of fungal diseases, including pathogens associated with *Botryosphaeria* dieback, Petri disease, and black foot disease, has been reported in several grape-producing areas along the coastal region [11,12].

The occurrence of this disease across different regions and over multiple years, together with the high plant mortality observed, underscores the importance of investigating its etiology. Disease outbreaks could be influenced by interactions between environmental conditions and host susceptibility; therefore, accurate identification of causal agents is essential for developing effective integrated disease management strategies.

Although this disease has been frequently observed in commercial vineyards, no study has established its causal pathogens in Peru. Furthermore, there are no reports describing similar and extensive belowground collar lesions in grapevines from other major table-grape-producing countries in South America. The objective of the present study was to identify the causal agent responsible for this rapid decline using a polyphasic approach. This involved morphological characterization, cardinal temperature assays to evaluate the pathogen's thermal response, and phylogenetic analyses based on the internal transcribed spacer (ITS) and histone H3 (*his3*) regions. Additionally, pathogenicity tests were conducted to confirm the aggressiveness of the isolates and validate their role in the observed decline. The results of this study will provide a basis for improved pathogen management and implementing appropriate measures.

2. Materials and Methods

2.1. Field Survey and Isolation

All symptomatic plants (1 to 2-year-old) were randomly selected from commercial orchards in the Piura and Ica regions from 2022 to 2025. Disease incidence was assessed by counting the number of symptomatic and dead plants in each affected field. At least two plants per orchard were collected and transported to the laboratory for further analyses.

The basal stem and root tissues of the rootstocks were washed with tap water and rinsed with sterile distilled water. Margins of the lesions from the collar tissues were dissected in longitudinal and cross-sections, and the bark was removed before cutting into 0.5–1 cm2 pieces. These segments, including sapwood tissues, were surface sterilized in 90% ethanol for 10 s, blotted dry on sterile filter papers, and transferred (five pieces per dish) to potato dextrose agar (PDA; HiMedia, Maharashtra, India) and CMA-PARP medium [13] amended with 0.02 g liter-1 benomyl (CMA-PARPB). The Petri dishes were incubated at 24 °C in the dark for 72 h and visually checked for developing colonies over seven days. Hyphal tips of the resultant colonies were subcultured on fresh PDA to obtain pure single-hyphal cultures and determine colony morphology.

 doi:10.20944/preprints202605.0304.v1

2.2. Morphological and Physiological Characterization

To determine the morphological characteristics of the isolates, they were plated onto potato dextrose agar (PDA) medium (HiMedia, Maharashtra, India) and incubated at 25 °C for 5 days under mixed white and near-UV light with a 12 h photoperiod. Measurements of the fungal structures were performed by removing an agar square from synthetic nutrient-poor agar (SNA) plates, placing it on a microscope slide, and adding a drop of water and a coverslip. Observations were performed using a Better Scientific Q190A-LCD microscope with differential interference contrast, and images were captured with the integrated 8MP digital camera. Thirty measurements were obtained for each structure.

Cardinal growth temperatures were determined by inoculating 90 mm diameter PDA plates with a 5 mm diameter plug cut from the edge of an actively growing fungal colony. Two representative isolates were used in this study: Three replicates of each isolate and temperature were prepared, and the experiment was performed twice. Colony growth was recorded after seven days in two orthogonal directions. Temperature growth experiments were performed at 5-40 °C in 5 °C intervals.

The effect of temperature on radial mycelial growth was modeled by fitting a second-degree polynomial regression ($y = ax^2 + bx + c$) to the growth data of each isolate, from which cardinal temperatures (T_{min}, T_{opt}, T_{max}) were derived analytically, the optimum as the vertex of the parabola ($T_{opt} = -b/2a$) and the minimum and maximum as the real roots of the fitted equation [14]. All analyses and visualizations were performed in R v. 4.x using the ggplot2 package [15].

2.3. DNA Extraction, PCR, and Sequencing

Selected fungal isolates: DVP-3 and DVI-16, obtained from symptomatic plant tissues and maintained as monosporic cultures for six days at 25 °C in the dark for subsequent molecular analyses, were used. Total DNA was extracted using the E.Z.N.A. Plant Miniprep Kit (Omega Bio-tek, Doraville, Georgia, USA) following the manufacturer's instructions. Before extraction, mechanical disruption of fungal mycelium was performed by adding four tungsten carbide beads (3 mm diameter) (Qiagen, Hilden, Germany) and homogenization in FastPrep-24 5G (MP Biomedicals, California, USA) at 5 m/s for 20s in two consecutive cycles.

2.4. PCR Amplification and Sequencing

Two gene regions of recognized taxonomic importance were amplified by polymerase chain reaction (PCR): the internal transcribed spacer region together with the 5.8S rRNA gene (ITS) using primers ITS1F (5′-CTTGGTCATTTAGAGGAAGTAA-3′)[16] and ITS4 (5′-TCCTCCGCTTATTGATATGC-3′) [17], and the histone H3 gene (*his3*) using primers CYLH3F (5′-AGGTCCACTGGTGGCAAG-3′) and CYLH3R (5′-AGCTGGATGTCCTTGGACTG-3′) [18]. Amplification reactions were performed in a Peltier Thermal Cycler-200 (MJ Research) under the following conditions: initial denaturation at 94 °C for 3 min, followed by 35 cycles of denaturation at 94 °C for 30 s, annealing at 55 °C for 30 s, elongation at 72 °C for 45 s, and a final extension at 72 °C for 10 min. The resulting PCR products were purified and bidirectionally sequenced by Macrogen Inc., Sequencing Center (The Netherlands, Europe), using the same primer pairs previously used, thereby ensuring the production of high-quality, intact sequences for subsequent phylogenetic analyses.

2.5. Phylogenetic Analyses

Consensus sequences were assembled using Sequencher v. 5.3 software (Gene Codes Corporation, Ann Arbor, Michigan, USA) and subsequently subjected to homology searches in the NCBI GenBank database using the Basic Local Alignment Search Tool (BLAST) to perform preliminary taxonomic identification. A comprehensive phylogenetic dataset of 30 sequences was compiled, including 19 reference sequences from the genus *Pleiocarpon* representing the three

 doi:10.20944/preprints202605.0304.v1

described species: *P. algeriense* (nine sequences from strains of Algeria and Italy), *P. strelitziae* (nine sequences from strains of Italy), and *P. livistonae* (one sequence from the strain of Sri Lanka). Eight sequences from phylogenetically related genera were included as outgroups, encompassing *Dactylonectria* (two species: *D. macrodidyma* and *D. torresensis*), *Cylindrocladiella* (two sequences of *C. peruviana*), *Ilyonectria* (two species: *I. capensis* and *I. palmarum*), *Thelonectria* (one sequence of *T. olida*), and *Thyronectria* (one sequence of *T. quercicola*). The species *Xenogliocladiopsis cypellocarpa* (CBS 133814) was used as an outgroup to root the phylogenetic trees. These reference sequences were selected based on recent phylogenetic studies of the Nectriaceae family [19,20], prioritizing sequences from type strains and representatives of proven taxonomic quality.

2.6. Sequence Alignment, Concatenated Analysis, and Phylogenetic Inference

Sequences were aligned in Geneious Prime [21] using the MAFFT v.7 algorithm [22], and the resulting alignments were trimmed with GBlocks v.0.91b [23] to remove ambiguously aligned regions at the 5′ and 3′ ends and prevent biases in phylogenetic inference. To maximize phylogenetic resolution and statistical power, a concatenated analysis was performed by combining the two molecular markers in Geneious Prime [21], yielding a final matrix of 30 sequences totaling 648 aligned characters (ITS: 365; *his3*: 283). Phylogenetic reconstruction was performed using Bayesian inference with the MrBayes plugin in Geneious Prime[21,24], applying the GTR+Γ (General Time Reversible with gamma distribution) nucleotide substitution model to account for rate heterogeneity across sites. Markov Chain Monte Carlo (MCMC) analyses were executed for 2,500,000 generations using four chains (three heated and one cold) with a heating parameter of 0.2 and sampling every 1,000 generations. The initial 50% of sampled trees were discarded as burn-in (1,250,000 generations), and convergence was confirmed by verifying that the average standard deviation of split frequencies fell below 0.01. The resulting consensus tree was rooted with *X. cypellocarpa*, and Bayesian posterior probabilities were calculated to evaluate node support, reporting only values ≥ 0.70 to ensure statistical robustness in phylogenetic interpretations.

2.7. Pathogenicity Tests

Pathogenicity tests were conducted in a greenhouse from December 2024 to April 2025. One-year-old dormant vines cv. Red Globe grafted onto Salt Creek (Ramsey, *Vitis champini*) rootstock were used as plant material. These had previously been exposed to thermotherapy (50 °C for 30 min). The treated plants grew in plastic pots (30 cm diameter × 40 cm depth) filled with a sterile potting mix (75% peat, 25% sand, vol/vol). Inoculations began when the plants developed an active 15-cm shoot. Two representative isolates of *Pleiocarpon* served as inoculum: DVP-3 (from grapevine collar rots in the Piura region) and DVI-16 (from grapevine collar rots in the Ica region). The experiment comprised two runs: the first from December 2024 to February 2025, and the second from February to April 2025.

Plants were inoculated by wounding. The procedure followed methods used for *Pleiocarpon* pathogenicity tests in grapevine[19], avocado[20], and other *Cylindrocarpon*-like asexual morphs on grapevine[25]. For each isolate, 20 plants were stem-inoculated 8 cm from the rootstock base. A 5-mm-diameter bark disk was removed using a cork borer to expose the cambium. A PDA agar disk of similar size, colonized by *Pleiocarpon* mycelium, was placed on the exposed cambium. After inoculation, the wound was moistened with sterile water and sealed with a Parafilm strip. The inoculated wounds of 20 plants per treatment were buried 8 cm deep in the substrate. Twenty control grapevine plants received uninfested PDA disks and were arranged as described above. The inoculated plants were kept on benches in a greenhouse and watered as needed. Greenhouse temperatures during the trial ranged from 26 °C to 32 °C. Symptoms of shoot wilt and other foliar changes were observed weekly.

After 6 weeks, plants from all treatments were removed from the pots to record lesions. The stem bark surface was scraped with a sterile scalpel. This revealed the margins between healthy and necrotic tissues, both above and below the inoculation point. The canker area was traced onto a transparent plastic sheet and then digitized. Quantification was done using Assess software

 doi:10.20944/preprints202605.0304.v1

(American Phytopathological Society, St. Paul, MN). The lesion area was calculated by subtracting the size of the inoculation wound. These data were used for statistical analyses.

To confirm that each inoculated *Pleiocarpon* isolate caused the lesions, small wood pieces were taken from the leading edges of the lesions. These were plated onto PDA medium to re-isolate the pathogen and confirm Koch's postulates.

2.8. Data Analysis

Analysis of variance was performed using a completely randomized design, with lesion area recorded for each *Pleiocarpon* isolate in the pathogenicity tests. Means were separated according to Fisher's least significant difference test ($P< 0.05$) using SAS statistical software version 9.0 (SAS Institute, Cary, NC, USA).

3. Results

3.1. Symptoms Description

Symptomatic plants were found on 1–2-year-old plantations. The first symptoms appeared as necrotic leaf margins on the oldest leaves. Affected vines soon showed sudden shoot wilting (Figure 1) and later, death of the aerial parts (Figure 1a, 1b). Diseased plants showed no internal lesions on the shoots, cordons, or stems above the graft union. To better understand these symptoms, the soil around the stem was removed to expose the rootstock collar and lateral roots. After removing the superficial tissues here, below-ground collar rots of varying extents became visible along the rootstock. Lesions began in the buried portion, spreading toward the graft union, and to the roots (Figure 1c). Within a few weeks, extensive areas of plants died after the initial symptoms (Figure 1d), requiring replanting. However, these new plants also died from the same disease in subsequent warm seasons.

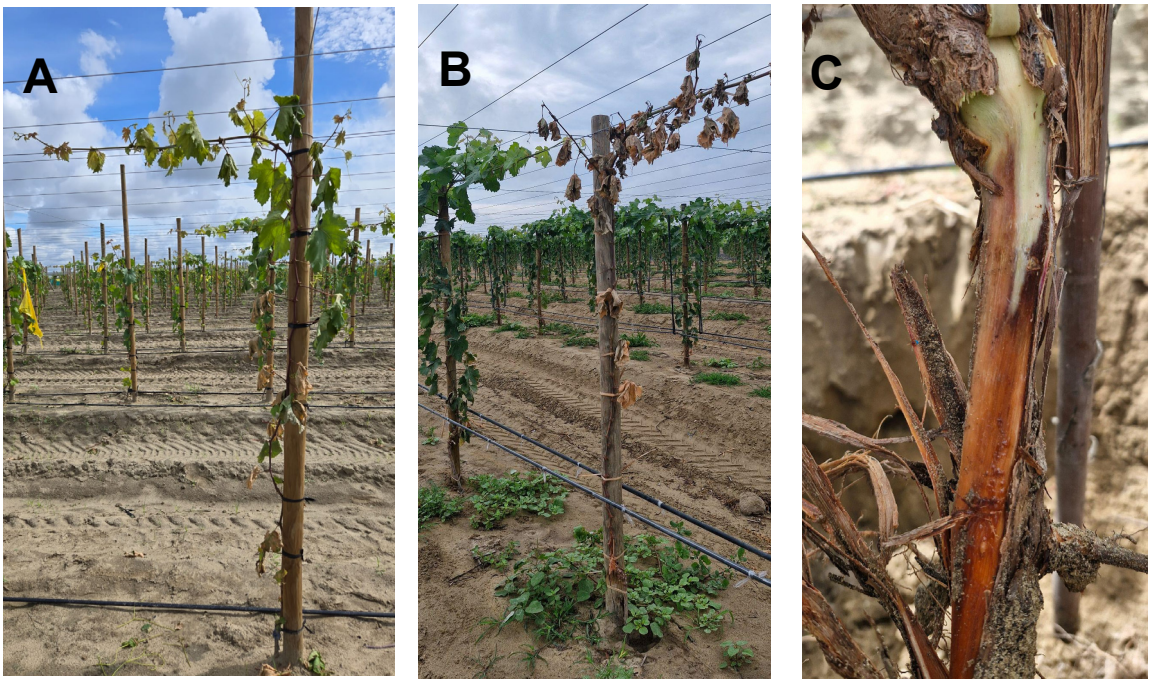

 doi:10.20944/preprints202605.0304.v1

Figure 1. Field symptoms, collar rot necrosis, and extensive plant mortality on young grapevines. **(A)** Early decline is characterized by leaf wilting and shoot dieback in a newly established vineyard. **(B)** Advanced decline with severe dieback and canopy collapse. **(C)** Below-ground collar rots along the rootstock after removal of the outer bark, dark brown discoloration of cortical and vascular tissues is visible at the crown and proximal roots, consistent with infection by *Pleiocarpon* sp. **(D)** Extensive plant mortality a few days after the onset of decline symptoms.

3.2. Field Survey and Isolations

Diseased plant samples (n = 64) were collected from 22 different grapevine commercial fields in the Piura region: Piura (12), Sullana (6), Morropón (2), and from two grapevine fields in the Ica region. Notably, approximately 95% of the symptomatic plants were from recent plantings, less than 1 year old. Furthermore, all symptomatic plants (100%) had Salt Creek as their rootstock.

A total of 44 fungal strains with similar characteristics were isolated from the infected plants. In 2022, the first known outbreak of this disease affected over 10% of plants. In 2023, six young commercial plantations experienced this syndrome. Disease incidence increased over time. In some vineyards, plant mortality reached up to 30%. Additionally, this disease first appeared, to a lesser extent, in the Ica region (southern Peru) in 2023. In 2024 and 2025, several other young commercial grapevine plantations were established. Symptomatic plants affected by this syndrome are commonly observed during late spring, summer, and early autumn (October-April).

3.3. Morphological and Physiological Characterization

Isolations from necrotic lesions of the collar rootstock consistently yielded a *Cylindrocarpon*-like anamorph, a group of fungi known to cause diseases such as black-foot disease in grapevines and other woody plants. It is important to note that no *Phytophthora* spp. or other previously reported grapevine pathogens were isolated in this study.

Morphological and physiological features of the isolates matched with previously described *Pleiocarpon* species. The mycelium was cottony, with an average density, on PDA. The surface was cinnamon to honey in color, with buff aerial mycelium. To expand upon these initial observations, the following mycological characteristics were documented for further comparative analysis.

Conidiophores were simple, arising laterally or terminally from aerial mycelium. These bore up to two monophialidic conidiogenous cells. Microconidia were abundant, aseptate, hyaline, and ellipsoidal to ovoid or subcylindrical. They were straight to slightly curved, with a clearly laterally displaced hilum. Macroconidia were cylindrical to subcylindrical, hyaline, straight to curved, and 2–5 septate. Chlamydospores were absent.

The results showed that mycelial growth of *Pleiocarpon* isolates DVP-3 and DVI-16 exhibited a unimodal response to temperature. Specifically, no growth was observed at 5 °C for DVP-3, whereas

 doi:10.20944/preprints202605.0304.v1

DVI-16 showed minimal development at this temperature. Growth increased progressively from 10 °C to 30 °C in both isolates, reaching a maximum at 30 °C. However, growth declined sharply at 35 and 40 °C (Figure 2).

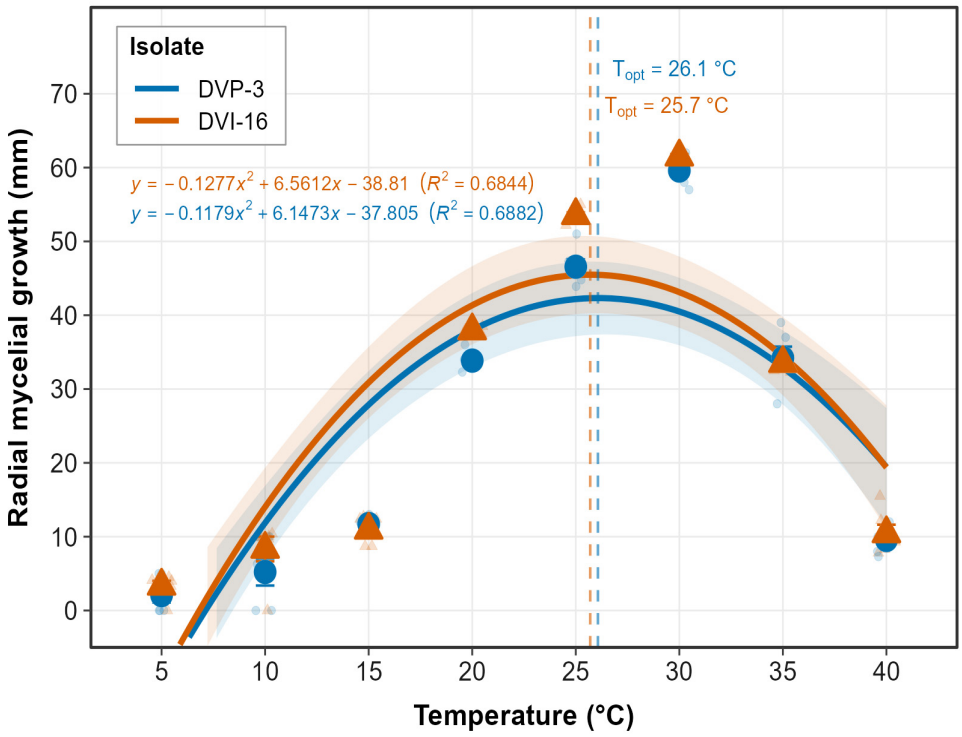

Figure 2. Influence of temperature on the radial mycelial growth of *Pleiocarpon* isolates DVP-3 and DVI-16. Data points represent the mean radial growth (mm) measured on potato dextrose agar (PDA) after 7 days of incubation at temperatures ranging from 5 to 40 °C. Dotted lines represent the fitted quadratic regression models. Calculated optimum temperatures (Topt): DVP-3 = 26.1 °C (95% CI: 25.1–28.3 °C); DVI-16 = 25.7 °C (95% CI: 24.7–27.7 °C).

Quadratic regression models adequately described the relationship between temperature (T, °C) and colony diameter (Y, mm). For isolate DVP-3, the fitted equation was Y =- 0.1179T² + 6.1473T - 37.805. The model showed good predictive accuracy (RMSE = 11.54 mm). The estimated optimal temperature (Topt) was 26.1 °C (95% CI: 25.1-28.3 °C). For isolate DVI-16, the fitted equation was Y =- 0.1277T² + 6.5612T - 38.810. This model also showed a solid fit (RMSE = 12.17 mm). The estimated Topt was 25.7 °C (95% CI: 24.7-27.7 °C).

Residual analyses indicated a symmetric distribution around zero. There was no evidence of heteroscedasticity or systematic deviation, indicating that the quadratic models are adequate within the evaluated thermal range. Both isolates exhibited similar calculated thermal optima near 26 °C. Maximum experimental growth was observed at 30 °C within the evaluated temperature range.

3.4. Molecular Identification and Phylogenetic Analysis

Bayesian phylogenetic analysis based on concatenated ITS and *his3* sequences resolved well-supported clades corresponding to the recognized *Pleiocarpon* species. The Peruvian isolates DVP-3 and DVI-16 were recovered as a distinct lineage, clustering as the sister taxon to the *P. strelitziae* clade with maximum posterior probability (PP = 1.00).

Although closely related to *P. strelitziae*, Peruvian isolates did not cluster within this species clade but formed an independent, well-supported branch, showing a clear phylogenetic separation (Figure 3). This topology suggests that the Peruvian isolates share a recent common ancestor with *P. strelitziae*

 doi:10.20944/preprints202605.0304.v1

while maintaining sufficient genetic divergence to warrant recognition as a separate taxonomic group.

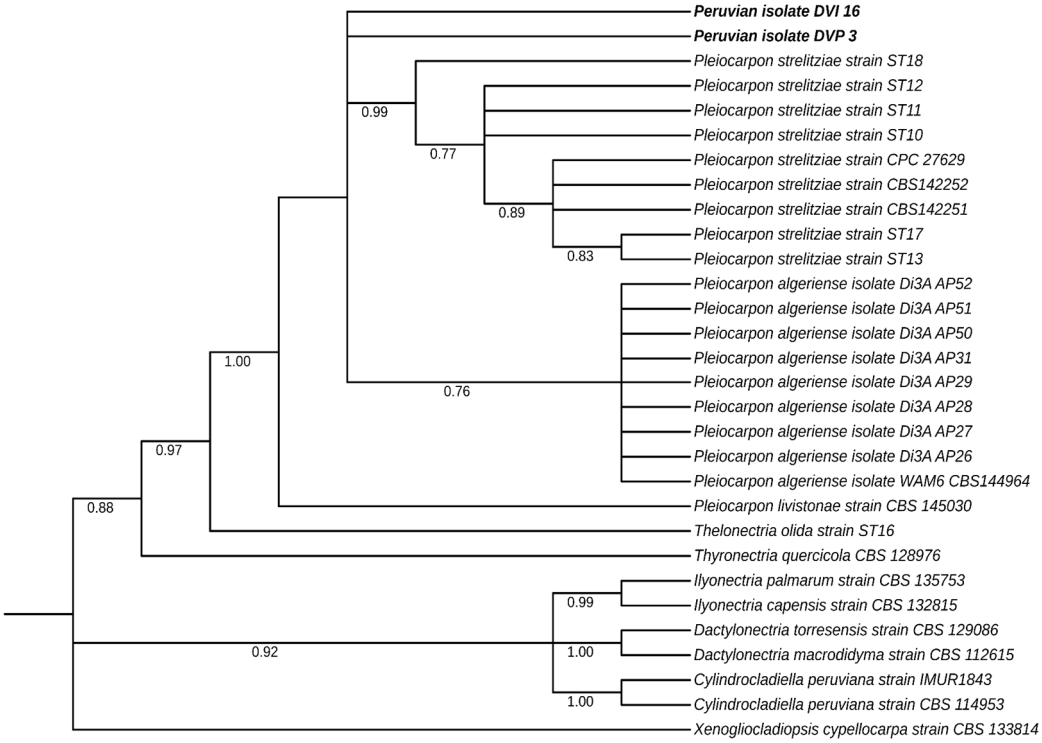

Figure 3. Bayesian phylogenetic tree inferred from concatenated ITS and *his3* sequences of *Pleiocarpon* sp. and related genera. The analysis was performed in MrBayes v3.2.6 under the GTR+Γ model with 2,500,000 MCMC generations, sampling every 1,000 generations; the first 1,250,000 generations were discarded as burn-in. Node labels indicate Bayesian posterior probabilities (PP ≥ 0.77). The tree is rooted with *Xenogliocladiopsis cypellocarpa.*

Other *Pleiocarpon* species, including *P. algeriense* and *P. livistonae*, formed distinct and well-supported clades, further corroborating the robustness of species-level resolution in the concatenated dataset. The short branch lengths within species clades, and longer branches separating major lineages, indicate low intraspecific but clear interspecific genetic variation.

3.4.1. Sequence Repository

Nucleotide sequences for DVP- 3 and DVI-16 isolates ITS (PZ158632, PZ158633) and *his3* (PZ234412, PZ234413) derived from this study were deposited in the NCBI GenBank database with their corresponding accession numbers to facilitate future comparative studies.

3.4.2. Pathogenicity Tests

All *Pleiocarpon* isolates tested were pathogenic to Salt Creek rootstock. In the first assay, DVP-3 caused shoot wilting in 2 of 20 plants at 35 days after inoculation (dai), increasing to 60% (12/20) by 42 dai, with declining symptoms. The DVI-16 isolate affected 7 of 20 plants (35%) at 42 dai. In the second assay at 42 dai, shoot wilting was observed in 85% (17/20) of plants with DVP-3 and 55% (11/20) with DVI-16.

On the assessment date for both trials, irregular dark lesions were observed on the wood under the bark, starting from the point of inoculation on the rootstocks. *Pleiocarpon* isolates were consistently recovered from all inoculated plants, thereby confirming the Koch postulates, whereas no isolates were recovered from negative controls in either trial.

The inoculation assays revealed statistically significant differences among the treatments in both experimental assessments; however, no statistically significant differences were detected between the two assayed isolates. In the first inoculation assay, treatment effects were highly significant (P =

 doi:10.20944/preprints202605.0304.v1

0.0001). In the second assay, the effects remained significant (P = 0.0032). This consistency showed a stable response pattern across the experiments.

At 42 dai, no lesions were observed in the control treatment (T0) in either assay, confirming the absence of disease under non-inoculated conditions. In contrast, treatments T1 (DVP-3) and T2 (DVI-16) developed measurable lesions. In the first assay, lesion areas reached 6.4 cm² for T1 and 5.7 cm² for T2; in the second, they increased slightly to 7.1 cm² and 6.3 cm², respectively.

According to the LSD test, both inoculated treatments differed significantly from the control; however, they did not differ significantly from each other, as indicated by the shared significance letters (Figure 4). This indicates that DVP-3 and DVI-16 exhibited similar levels of aggressiveness or similar pathogenic responses under the evaluated conditions.

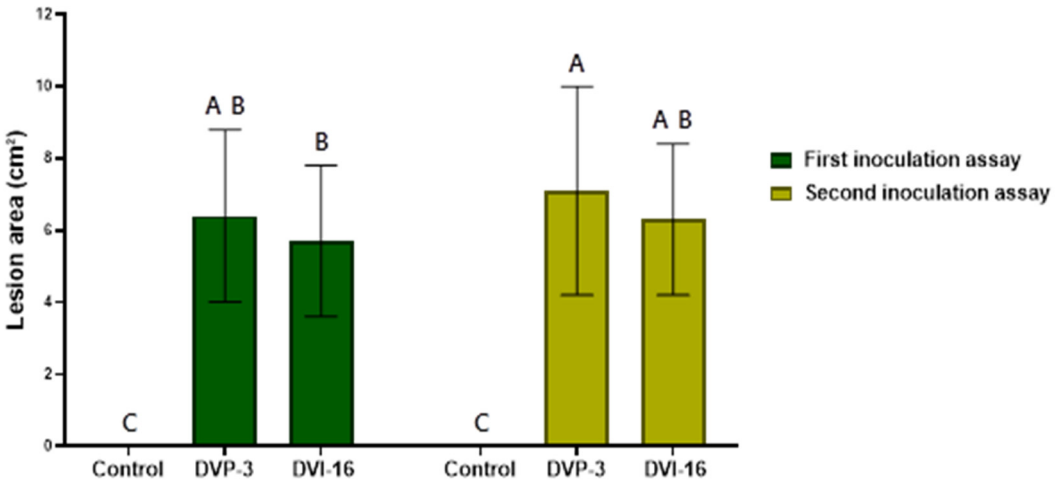

Figure 4. Pathogenicity of *Pleiocarpon* isolates DVP-3 and DVI-16 on grapevine rootstock Salt Creek (Ramsey - *Vitis champini*) under greenhouse conditions. Bars represent the mean lesion area (cm²) from two independent assays (n=20 per treatment). Error bars indicate the standard deviation. Means followed by the same letter are not significantly different according to Fisher's protected LSD test ($p < 0.05$). Control plants (T0) were inoculated with non-infested PDA disks and did not develop any symptoms.

The average lesion area increased from 4.0 cm² in the first assay to 4.4 cm² in the second assay, reflecting consistent disease expression across experiments. Furthermore, the coefficients of variation were low to moderate (7.67% and 12.60%), indicating acceptable experimental exactness and measurement reliability.

4. Discussion

This study documents a severe and recurrent decline of young grapevines in commercial vineyards in Peru. The disease is associated with belowground collar rots caused by an aggressive, phylogenetically distinct *Pleiocarpon* lineage. Notably, the syndrome represents an atypically severe form of black-foot disease, distinguished by rapid plant mortality soon after vineyard establishment. It occurs especially in plantings conducted during the warmest months (November-March) and results in a major economic impact, including plant loss, vineyard replanting, and reduced stand uniformity.

Key findings show that field observations, morphological analysis, cardinal-temperature testing, multilocus phylogenetic inference, and pathogenicity assays implicate a formerly unknown *Pleiocarpon* lineage as the causal agent of this emerging decline syndrome.

Typically, black-foot disease is associated with soilborne fungi in the Nectriaceae, including *Campylocarpon, Cylindrocladiella, Cylindrodendrum, Dactylonectria, Ilyonectria, Neonectria, Thelonectria*, and *Pleiocarpon* [19,26]. These fungi generally infect roots and basal tissues, causing necrosis, reduced root biomass, stunted growth, chlorosis, and eventually vine death [27–29]. However, the main

 doi:10.20944/preprints202605.0304.v1

evidence of our study is that collar rots observed were more extensive and rapidly lethal than previously reported, denoting a more aggressive disease phenotype associated with this pathogen.

The significance of *Pleiocarpon* as a pathogen is emphasized by its impact on diverse cropping systems. For example, *P. strelitziae* was first described, causing basal stem and root rot of *Strelitzia reginae* in Italy [30], and *P. algeriense*, initially isolated and described from grapevine nurseries in Algeria [19], was later reported as the causal agent of stem and crown rot of avocado (*Persea americana*) under field conditions [20]. These reports emphasize the genus's capacity to induce extensive necrosis, structural collapse of crown tissues, and rapid plant death. In the context of our research, the present study expands the documented host-pathogen interaction of *Pleiocarpon* to commercial grapevines in South America and supports the presence of a distinct lineage associated with severe vineyard decline.

To further characterize the pathogen, phylogenetic analyses based on concatenated ITS and *his3* loci consistently resolved the Peruvian isolates within *Pleiocarpon*, with the isolates DVP-3 and DVI-16 forming a well-supported sister lineage to *P. strelitziae*. Topological congruence across single-locus phylogenies further supports genealogical exclusivity. Such phylogenetic structure is consistent with patterns detected in other pathogens associated with black-foot, in which geographically structured lineages often correspond to cryptic species diversity [19,31]. Although formal taxonomic description is beyond the scope of this work, molecular evidence strongly suggests the presence of a separate evolutionary lineage.

These phylogenetic results are informed by the molecular tools chosen. Within *Cylindrocarpon*-like fungi, ITS sequences alone frequently provide insufficient resolution to delimit species boundaries, mainly within genera characterized by high morphological conservatism and cryptic diversity [31–33]. The histone H3 gene (*his3*) has proven to be a more discriminating marker for this group: in the study establishing *Pleiocarpon* as a distinct genus, *his3* was the locus that resolved *P. algeriense* and *P. strelitziae* as separate lineages, whereas LSU and rpb2 failed to separate them[19]. Moreover, the usefulness of this marker extends to routine species identification: Akgül et al. [34] characterized seven black-foot species across four genera in Turkish nurseries using *his3* as the sole molecular marker, employing the same CYLH3F/CYLH3R primer pair used in the present study. This demonstrates that this locus provides species-level discrimination sufficient for applied diagnostic and epidemiological purposes. Accordingly, in the present work, the combination of ITS and *his3* into a concatenated dataset strengthened phylogenetic inference beyond what either marker could achieve independently, recovering the Peruvian isolates as a well-supported lineage sister to *P. strelitziae* with maximum posterior probability.

An important factor modulating disease severity is rootstock genotype. In Peru, commercial table grape production relies almost exclusively on Salt Creek (Ramsey, *Vitis champini*) rootstock. Initially, diverse rootstocks were introduced as table grape expansion began in Peru, but only Salt Creek met the industry's favorable conditions for growth. Salt Creek is favored for its tolerance to salinity, sandy soils, drought, and nematodes, as well as its compatibility with commercial scions and increased final yield [35–37]. However, the near-exclusive use of this single susceptible rootstock likely increases disease incidence and regional spread, thereby creating a structurally vulnerable production system.

All tested *Pleiocarpon* isolates were pathogenic to Salt Creek rootstock, indicating host susceptibility. Although our objective was to confirm pathogenicity and not replicate field epidemiology, the wound method was appropriate for this purpose. Black-foot pathogens infect basal tissues mainly through wounds caused by grafting, transplanting, or early root growth. Artificial wounding simulates natural infection courts and reduces variability.

Similar aggressiveness among tested isolates from different regions indicates that host and environmental aspects are more influential than isolate-specific variation. Repeated collar infections in buried basal tissues imply that soil moisture is necessary for infection, while soil temperature plays the key role in syndrome onset. Together, these factors explain rapid disease progression and high mortality.

 doi:10.20944/preprints202605.0304.v1

Seasonal context further explains these dynamics. In Peru, new vineyards are established between October and February, when elevated soil and air temperatures promote rapid vine growth. This rapid growth allows plants to develop and quickly enter production at the next pruning. However, these ideal conditions for young plant growth also coincide with the period of greatest pathogen aggressiveness.

Consistent with this, the estimated optimal growth temperatures for *Pleiocarpon* isolates (Topt 25.7-26.1 °C) indicate adaptation to warm temperate conditions (Talley et al., 2002), and rapid mycelial growth at these temperatures may enhance colonization efficiency and infection success [38]. Maximum mycelial growth occurred at approximately 30 °C, further suggesting that the pathogens are tolerant of elevated soil temperatures typical of Peru's coastal grape-growing regions during vineyard establishment.

The epidemiology of this pathogen remains poorly understood, due in part to the lack of long-term survival structures, such as chlamydospores. As a result, infected nursery material serves as the primary inoculum source, pointing out the importance of transplant-associated wounds. Its spread across major grape-growing regions can be explained by the exchange of plant material among production areas, with infected nursery stock being a well-documented pathway for the dissemination of black-foot pathogens [39].

The origin of this *Pleiocarpon* lineage remains unknown and needs further investigation. Its aggressiveness and direct link to severe vineyard establishment failures and recurrent infections are concerning, particularly when a single rootstock is used under warm, arid conditions. Consequently, there is a need for optimized diagnostic protocols. Early detection and accurate identification are important to prevent dissemination through planting material and mitigate vineyard losses. To resolve these challenges, integrated disease management should focus on pathogen-free planting material, nursery hygiene, diversified rootstocks, and stress-reducing cultural practices. Additionally, establishing thermal thresholds could improve risk assessment and disease management in climate-conducive scenarios.

Supplementary Materials: The following supporting information can be downloaded at the website of this paper posted on Preprints.org, Figure S1: title; Table S1: title.

Author Contributions: Luis A. Álvarez: Writing – review & editing, Formal analysis, Funding acquisition, Supervision, Project administration. Gabriela Salcedo-Astorima: Writing – review & editing, Visualization; Investigation. Phillip Ormeño-Vásquez: Writing – review & editing, Conceptualization, Methodology. Naysha Rojas-Villa: Conceptualization, Methodology, Writing – original draft, Supervision, Project administration. Jose Soto-Heredia: Software, Validation, Data curation.

Funding: This research was supported by the National University of Cañete (Universidad Nacional de Cañete). In addition, the financial contribution of some authors is acknowledged, which helped to broaden the scope of the research studies.

Institutional Review Board Statement: Ethical review and approval were waived for this study due to the research involving only environmental soil samples, fungal microorganisms, and plant material. No human subjects or vertebrate animals were used in this investigation. All soil and plant sampling was conducted in accordance with local environmental regulations.

Informed Consent Statement: Not applicable.

Data Availability Statement: The datasets generated and analyzed during the current study are available from the corresponding author upon reasonable request. Raw sequencing data supporting the molecular identification results have been deposited in GenBank.

Acknowledgments: The authors wish to thank Foliumlab laboratory for the facilities provided for the isolation of some samples in the Ica area.

 doi:10.20944/preprints202605.0304.v1

Conflicts of Interest: The authors declare no conflicts of interest. The funders had no role in the design of the study; in the collection, analyses, or interpretation of data; in the writing of the manuscript; or in the decision to publish the results.

Abbreviations

The following abbreviations are used in this manuscript:

DAI	Days After Inoculation
PCA	Principal Component Analysis
ITS	Internal Transcribed Spacer
his3	Histone H3
PDA	Potato Dextrose Agar
PCR	Polymerase Chain Reaction
ANOVA	Analysis of Variance
SE	Standard Error
DNA	Deoxyribonucleic Acid

References

1. Palma, J.C.; Fabián-Campos, J.; Dioses-Morales, J.J.; Arias-Durand, A.D.; Espinoza-Córdova, G.; Gonzales-Uscamayta, M.; Rengifo-Maravi, J.C.; Chire-Murillo, E.T.; Caro Sánchez-Benites, V.A.; Jorge-Montalvo, P.; et al. Pisco, an Appellation of Origin from Peru: A Review. *Heliyon* **2025**, *11*, e42251, doi:10.1016/j.heliyon.2025.e42251.
2. USDA Foreign Agricultural Service *Fresh Deciduous Fruit Annual - Peru*; 2025;
3. PROVID Peru Exported 81,424,326 Boxes of Table Grapes.
4. Astudillo-Calderón, S.; Tello, M.L.; De Robador, J.M.A.; Pintos, B.; Gómez-Garay, A. First Report of *Fusarium equiseti* Causing Vascular Wilt Disease on Vitis Vinifera in Spain. *https://doi.org/10.1094/PDIS-01-19-0067-PDN* **2019**, *103*, doi:10.1094/PDIS-01-19-0067-PDN.
5. Úrbez-Torres, J.R.; Haag, P.; Bowen, P.; O'Gorman, D.T. Grapevine Trunk Diseases in British Columbia: Incidence and Characterization of the Fungal Pathogens Associated with Esca and Petri Diseases of Grapevine. *Plant Dis.* **2013**, *98*, 469–482, doi:10.1094/PDIS-05-13-0523-RE.
6. Akgül, D.S.; Önder, S.; Savaş, N.G.; Yıldız, M.; Bülbül, İ.; Özarslandan, M. Molecular Identification and Pathogenicity of *Fusarium* Species Associated with Wood Canker, Root and Basal Rot in Turkish Grapevine Nurseries. *Journal of Fungi* **2024**, *10*, 444, doi:10.3390/JOF10070444/S1.
7. Spies, C.F.J.; Mazzola, M.; McLeod, A. Characterisation and Detection of *Pythium* and *Phytophthora* Species Associated with Grapevines in South Africa. *European Journal of Plant Pathology 2011 131:1* **2011**, *131*, 103–119, doi:10.1007/S10658-011-9791-5.
8. Vázquez-Rowe, I.; Torres-García, J.R.; Cáceres, A.L.; Larrea-Gallegos, G.; Quispe, I.; Kahhat, R. Assessing the Magnitude of Potential Environmental Impacts Related to Water and Toxicity in the Peruvian Hyper-Arid Coast: A Case Study for the Cultivation of Grapes for Pisco Production. *Science of The Total Environment* **2017**, *601–602*, 532–542, doi:10.1016/J.SCITOTENV.2017.05.221.
9. Songy, A.; Fernandez, O.; Clément, C.; Larignon, P.; Fontaine, F. Grapevine Trunk Diseases under Thermal and Water Stresses. *Planta 2019 249:6* **2019**, *249*, 1655–1679, doi:10.1007/S00425-019-03111-8.
10. Hrycan, J.; Hart, M.; Bowen, P.; Forge, T.; Úrbez-Torres, J.R. Grapevine Trunk Disease Fungi: Their Roles as Latent Pathogens and Stress Factors That Favour Disease Development and Symptom Expression. *Phytopathol. Mediterr.* **2020**, *59*, 395–424, doi:10.14601/PHYTO-11275.
11. Alvarez, L.A.; Tamayo, D.; Castilla, C.; Munive, J.; Agustí-Brisach, C.; Gramaje, D.; Armengol, J. Occurrence of Grapevine Trunk Pathogens in Nurseries and Vineyards in the Northern and Southern Coast of Peru. In Proceedings of the Proc. 8th International Workshop on Grapevine Trunk Diseases; Valencia, June 18 2012.

 doi:10.20944/preprints202605.0304.v1

12. Munive, J.; Tamayo, D.; Castilla, P.C.; Agustí-Brisach, C.; Gramaje, D.; Armengol, J.; Alvarez, L.A. Wood-Inhabiting Fungi Associated with Grapevine Infections in Nurseries and Vineyards in Peru. In Proceedings of the Proceedings of the XXII Peruvian Congress of Phytopathology and XVII Latin American Congress of Phytopathology; Lambayeque, 2013.
13. Jeffers, S.N.; Martin, S.B. Comparison of Two Media Selective for *Phytophthora* and *Pythium* Species. *Plant Dis.* **1986**, *70*, 1038–1043.
14. Brennan, J.M.; Fagan, B.; Van Maanen, A.; Cooke, B.M.; Doohan, F.M. Studies on in vitro Growth and Pathogenicity of European Fusarium Fungi. *Eur. J. Plant Pathol.* **2003**, *109*, 577–587.
15. Wickham, H. *Ggplot2: Elegant Graphics for Data Analysis*; Springer-Verlag, Ed.; 2nd ed.; Springer International Publishing: Cham, 2016;
16. GARDES, M.; BRUNS, T.D. ITS Primers with Enhanced Specificity for Basidiomycetes - Application to the Identification of Mycorrhizae and Rusts. *Mol. Ecol.* **1993**, *2*, 113–118, doi:10.1111/J.1365-294X.1993.TB00005.X;WGROUP:STRING:PUBLICATION.
17. White, T.J.; Bruns, T.; Lee, S.; Taylor, J.W. Amplification and Direct Sequencing of Fungal Ribosomal RNA Genes for Phylogenetics. In *PCR Protocols: A Guide to Methods and Applications*.; Academic Press: San Diego, 1990; pp. 315–322.
18. Crous, P.W.; Groenewald, J.Z.; Risède, J.-M.; Simoneau, P.; Hywel-Jones, N.L. *Calonectria* Species and Their *Cylindrocladium* Anamorphs: Species with Sphaeropedunculate Vesicles. *Stud. Mycol.* **2004**, *50*, 415–430.
19. Aigoun-Mouhous, W.; Elena, G.; Cabral, A.; León, M.; Sabaou, N.; Armengol, J.; Chaouia, C.; Mahamedi, A.E.; Berraf-Tebbal, A. Characterization and Pathogenicity of *Cylindrocarpon*-like Asexual Morphs Associated with Black Foot Disease in Algerian Grapevine Nurseries, with the Description of *Pleiocarpon algeriense* Sp. Nov. *European Journal of Plant Pathology 2019 154:4* **2019**, *154*, 887–901, doi:10.1007/S10658-019-01708-Z.
20. Aiello, D.; Gusella, G.; Vitale, A.; Guarnaccia, V.; Polizzi, G. *Cylindrocladiella peruviana* and *Pleiocarpon algeriense* Causing Stem and Crown Rot on Avocado (*Persea Americana*). *European Journal of Plant Pathology 2020 158:2* **2020**, *158*, 419–430, doi:10.1007/S10658-020-02082-X.
21. Kearse, M.; Moir, R.; Wilson, A.; Stones-Havas, S.; Cheung, M.; Sturrock, S.; Buxton, S.; Cooper, A.; Markowitz, S.; Duran, C.; et al. Geneious Basic: An Integrated and Extendable Desktop Software Platform for the Organization and Analysis of Sequence Data. *Bioinformatics* **2012**, *28*, 1647–1649, doi:10.1093/BIOINFORMATICS/BTS199.
22. Katoh, K.; Standley, D.M. MAFFT Multiple Sequence Alignment Software Version 7: Improvements in Performance and Usability. *Mol. Biol. Evol.* **2013**, *30*, 772–780, doi:10.1093/MOLBEV/MST010.
23. Castresana, J. Selection of Conserved Blocks from Multiple Alignments for Their Use in Phylogenetic Analysis. *Mol. Biol. Evol.* **2000**, *17*, 540–552, doi:10.1093/OXFORDJOURNALS.MOLBEV.A026334.
24. Ronquist, F.; Huelsenbeck, J.P. MrBayes 3: Bayesian Phylogenetic Inference under Mixed Models. *Bioinformatics* **2003**, *19*, 1572–1574, doi:10.1093/BIOINFORMATICS/BTG180.
25. Carlucci, A.; Lops, F.; Mostert, L.; Halleen, F.; Raimondo, M.L. Occurrence Fungi Causing Black Foot on Young Grapevines and Nursery Rootstock Plants in Italy. *Phytopathol. Mediterr.* **2017**, *56*, 10–39, doi:10.14601/PHYTOPATHOL_MEDITERR-18769.
26. Fontaine, F.; Trouillas, F.P.; Armengol, J.; Eskalen, A. Fungal Trunk Diseases: A Global Threat to Grapevines. *Annu. Rev. Phytopathol.* **2025**, *63*, 577–602, doi:10.1146/ANNUREV-PHYTO-121323-022259/CITE/REFWORKS.
27. Hallenn, F.; Crous, P.W.; Fourie, P. h. A Review of Black Foot Disease of Grapevine. *Phytopathologia mediterranea. Volume 45, Supplement, 2006* **2006**, 1000–1013, doi:10.1400/52261.
28. Agustí-Brisach, C.; Armengol, J. Black-Foot Disease of Grapevine: An Update on Taxonomy, Epidemiology and Management Strategies. *Phytopathol. Mediterr.* **2013**, *52*, 245–261.
29. Gramaje, D.; Urbez-Torres, J.R.; Sosnowski, M.R. Managing Grapevine Trunk Diseases With Respect to Etiology and Epidemiology: Current Strategies and Future Prospects. *https://doi.org/10.1094/PDIS-04-17-0512-FE* **2017**, *102*, 12–39, doi:10.1094/PDIS-04-17-0512-FE.

 doi:10.20944/preprints202605.0304.v1

30. Aiello, D.; Polizzi, G.; Crous, P.W.; Lombard, L. *Pleiocarpon* Gen. Nov. and a New Species of *Ilyonectria* Causing Basal Rot of Strelitzia Reginae in Italy. *IMA Fungus* **2017**, *8*, 65–76, doi:10.5598/IMAFUNGUS.2017.08.01.05/FIGURES/5.
31. Lawrence, D.P.; Nouri, M.T.; Trouillas, F.P. Taxonomy and Multi-Locus Phylogeny of *Cylindrocarpon*-like Species Associated with Diseased Roots of Grapevine and Other Fruit and Nut Crops in California. *Fungal Syst. Evol.* **2019**, *4*, 59–75, doi:10.3114/FUSE.2019.04.06.
32. Cabral, A.; Rego, C.; Nascimento, T.; Oliveira, H.; Groenewald, J.Z.; Crous, P.W. Multi-Gene Analysis and Morphology Reveal Novel *Ilyonectria* Species Associated with Black Foot Disease of Grapevines. *Fungal Biol.* **2012**, *116*, 62–80, doi:10.1016/J.FUNBIO.2011.09.010.
33. Mora-Sala, B.; Cabral, A.; León, M.; Agustí-Brisach, C.; Armengol, J.; Abad-Campos, P. Survey, Identification, and Characterization of *Cylindrocarpon*-Like Asexual Morphs in Spanish Forest Nurseries. *https://doi.org/10.1094/PDIS-01-18-0171-RE* **2018**, *102*, 2083–2100, doi:10.1094/PDIS-01-18-0171-RE.
34. Akgül, D.S.; Yıldız, M.; Güngör Savaş, N.; Bülbül, İ.; Özarslandan, M.; Leon, M.; Armengol, J. Occurrence and Diversity of Black-Foot Pathogens on Asymptomatic Nursery-Produced Grapevines in Turkiye. *European Journal of Plant Pathology 2022 164:1* **2022**, *164*, 21–32, doi:10.1007/S10658-022-02535-5.
35. Suarez, D.L.; Celis, N.; Anderson, R.G.; Sandhu, D. Grape Rootstock Response to Salinity, Water and Combined Salinity and Water Stresses. *Agronomy 2019, Vol. 9, Page 321* **2019**, *9*, 321, doi:10.3390/AGRONOMY9060321.
36. Zasada, I.A.; Howland, A.D.; Peetz, A.B.; East, K.; Moyer, M. Vitis Spp. Rootstocks Are Poor Hosts for Meloidogyne Hapla, a Nematode Commonly Found in Washington Winegrape Vineyards. *Am. J. Enol. Vitic.* **2019**, *70*, 1–8, doi:10.5344/AJEV.2018.18027.
37. Elaidy, A.A.; Abo-Ogiala, A.M.; Khalf, I.R. Effect of Different Grape Rootstocks on the Growth, Yield and Quality of Superior Grape under Salt Stress. *Middle East Journal of Agriculture Research* **2019**, *8*, 167–175.
38. Garrett, K.A.; Dendy, S.P.; Frank, E.E.; Rouse, M.N.; Travers, S.E. Climate Change Effects on Plant Disease: Genomes to Ecosystems. *Annu. Rev. Phytopathol.* **2006**, *44*, 489–509, doi:10.1146/ANNUREV.PHYTO.44.070505.143420/CITE/REFWORKS.
39. Gramaje, D.; Armengol, J. Fungal Trunk Pathogens in the Grapevine Propagation Process: Potential Inoculum Sources, Detection, Identification, and Management Strategies. *https://doi.org/10.1094/PDIS-01-11-0025* **2011**, *95*, 1040–1055, doi:10.1094/PDIS-01-11-0025.